ISSN: 2688-8645

A Novel Optimization Method for Electric Capacitated Vehicles Routing Problem Considering Battery Degradation Based on Hybrid Neighborhood Search Algorithm

Zongao Zhang, Qian Wang *, Jun Jiang, Xiaoyu Liu, Jinnan Yu

School of Navigation and Shipping, Shandong Jiaotong University, Jinan, Shandong 264209, China

* Corresponding Author: Qian Wang

Abstract

With the growing adoption of electric vehicles in logistics, the electric capacitated vehicle routing problem has become increasingly important. The battery, as a core component of electric vehicles, directly affects operational costs due to its degradation over time. Therefore, incorporating battery degradation into vehicle routing optimization is essential. This study incorporates battery degradation cost into the objective function, establishing a comprehensive mathematical model that further reduces overall transportation costs. Meanwhile, a hybrid genetic neighborhood search algorithm is developed by introducing the operator mechanism of neighborhood search into the genetic algorithm framework. This integration accelerates convergence and improves solution quality by combining the global search capability of genetic algorithms with the local refinement strength of neighborhood search. Numerical experiments demonstrate the effectiveness of the proposed algorithm, offering valuable insights and guidance for optimizing electric vehicle routing problems under realistic operational conditions.

Keywords

Electric Capacitated Vehicle Routing Problem; Battery Degradation; Hybrid Genetic Neighborhood Search Algorithm.

1. Introduction

Due to new policies and regulations related to greenhouse gas emissions in the transportation industry, logistics companies are paying higher fines for every gram of carbon dioxide emissions per kilometer [1]. To mitigate this issue, one effective way to reduce greenhouse gas emissions is to replace fuel-powered vehicles with electric vehicles (EVs) [2]. This is particularly relevant in key logistics hubs such as ports and their surrounding areas, where traditional fuel-powered vehicles face both efficiency and cost challenges [3]. The growing adoption of EVs as a viable alternative to reduce energy consumption and enhance transportation efficiency in port logistics has attracted significant attention to the electric capacitated vehicle routing problem (ECVRP) [4]. Compared with conventional fuel-powered vehicles, EVs present unique operational constraints, such as limited battery capacity and extended charging times. As a result, these factors increase the complexity of path optimization [5].

At present, EVs primarily utilize lithium batteries as their main power source, offering advantages such as higher energy efficiency, longer lifespan, and extended driving range [6]. However, after 5-8 years of operation, or when the battery capacity degrades to approximately 70% of its initial capacity, replacement becomes necessary to ensure safe and reliable performance [7]. Consequently, battery degradation emerges as a critical factor to be considered in the ECVRP.

The Vehicle Routing Problem (VRP), initially proposed by Dantzig and Ramser [8], has evolved over six decades into numerous variants, including capacitated VRP and VRP with time windows. These studies aim to address transportation efficiency and cost reduction in real-world logistics systems [9-10]. In recent years, driven by the rise of low-carbon economies and green logistics, electric vehicle routing problem (EVRP) has garnered significant attention. Research focus has shifted from single-objective optimization, for example, shortest path or minimal travel time, to multi-objective frameworks integrating energy consumption and environmental impact [11]. As an extension of traditional VRP tailored for electric vehicles, EVRP emphasizes optimizing route planning to reduce energy consumption, minimize carbon emissions, and enhance transportation efficiency. With the growing adoption of EVs in logistics, EVRP has emerged as a critical research area, particularly in balancing operational demands with energy and environmental sustainability [12]. To further explore the application of battery degradation and heuristic algorithms in ECVRP, this study reviews relevant literature to establish a solid theoretical foundation and inform practical applications.

In the ECVRP aspect, Schneider et al. established benchmark instances for EVRP with time windows based on Solomon datasets, employing a hybrid metaheuristic combining variable neighborhood search (VNS) and tabu search [13-14]. He et al. investigated optimal placement of public EV charging stations in Beijing, demonstrating the superiority of the P-median model over classical location-allocation approaches [15]. Sadati et al. proposed a flexible delivery EVRP model allowing customers to specify multiple time windows and delivery locations [16]. Erdelić compared single-charge versus multi-charge strategies for EV fleets, revealing trade-offs in operational flexibility and energy management [17]. Lu et al. introduced the time-dependent EVRP, incorporating charging decisions and traffic congestion dynamics, and validated their model using VNS-based solutions [18]. Mao et al. extended EVRP to scenarios with heterogeneous charging options and evaluated improved ant colony optimization algorithms for multi-objective optimization [19]. Wang et al. addressed a multi-depot EVRP with time windows and shared charging stations, developing a collaborative optimization framework validated via case studies in Chongqing [20].

In the battery degradation aspect, Liu et al. proposed a multi-objective optimization model from the EV user perspective, integrating electricity cost and battery degradation, and empirically validated the impact of charging profiles on battery lifespan [21]. Wang et al. introduced an inverse-order matching strategy for electric bus fleets, incorporating a battery degradation model to predict capacity loss and optimize replacement schedules [22]. Li et al. proposes a convolutional neural networks and the informer model that integrates battery characteristics and driving behavior from discharge sequence features to accurately predict electric vehicle battery capacity degradation in real-world scenarios [23]. Yu et al. proposed a battery degradation mitigation-oriented charging and order-serving problem for EVs operating on the e-hailing platform, to maximize the lifespan profit for individual EVs [24]. Ou developed a battery degradation model for electric vehicles, which simulates the impact of various energy management modules on battery capacity degradation [25].

In the heuristic algorithms aspect, Zhang et al. enhanced fuzzy simulation with an adaptive large neighborhood search algorithm, embedding variable neighborhood descent to solve fuzzy EVRP with time windows and charging stations [26]. Hien et al. proposed a clustering-inspired greedy search algorithm hybridized with genetic algorithms (GA), termed GSGA, for tram routing optimization [27]. Souza et al. developed a flexible variable neighborhood search framework for classical EVRP and battery-swapping station location-routing problems [28]. Duman et al. designed a bidirectional pulse algorithm with pruning strategies to address pricing subproblems in flexible delivery EVRP [29]. Yang et al proposed a hybrid adaptive large

ISSN: 2688-8645

neighborhood search heuristic algorithm for solving the electric vehicle routing problem considering time windows, mobile charging, and nonlinear battery degradation [30]. İslim et al. combined the variable neighborhood search algorithm with an exact solver to solve the electric travel salesman problem with time window [31].

While existing studies have addressed the fundamental challenges of electric vehicle routing, critical factors such as battery degradation costs remain relatively underexplored. Neglecting these factors leads to suboptimal routing strategies, higher operational expenses, and accelerated battery degradation, ultimately undermining the economic and environmental advantages of electrified logistics systems.

This study proposes a hybrid genetic neighborhood search algorithm (HGNSA) to minimize total transportation costs by integrating battery degradation into the ECVRP framework. The main contributions of this study are summarized as follows.

First, a cost model is developed that quantifies battery degradation cost based on cumulative battery throughput and depth of discharge, and incorporates the resulting degradation cost directly into the total logistics cost function.

Second, HGNSA algorithm is proposed, combining the global exploration capability of genetic algorithms with local refinement through four neighborhood operators. The method enhances solution quality and convergence speed.

Third, numerical experiments on benchmark instances validate the effectiveness and stability of the proposed algorithm. Results demonstrate that HGNSA achieves lower logistics costs compared to classical genetic algorithms, especially under battery degradation scenarios.

The rest of this study is organized as follows: Section 2 presents the problem definition and mathematical formulation. Section 3 introduces the proposed HGNSA, including the encoding scheme, selection, crossover, mutation, and neighborhood search strategies. Section 4 provides numerical experiments and results. Conclusions of this study are given in Section 5.

2. Problem Statement

2.1. Problem Description and Notation

The ECVRP is a variant of the capacitated vehicle routing problem (CVRP), where deliveries are performed by EVs. It aims to optimize delivery routes under dual constraints of limited battery capacity and vehicle load capacity. A key characteristic of EVs is that they operate using battery-stored electric energy rather than fuel. When an EV's remaining battery charge falls short of reaching the next customer node or any charging station, the vehicle travels to the nearest charging station for a full recharge.

The ECVRP problem is described on weighted graphs with vertex sets. is the set of nodes which represent the central depot , the customers , the vehicles and charging stations . represents the set of arcs.

To balance model fidelity and computational tractability, we simplify the mathematical framework under the following assumptions.

(1) Each customer is fully served by a single vehicle, and split deliveries are not allowed.

(2) The central depot and charging stations are fixed at known locations. Customer nodes, their spatial coordinates, and demand values are predetermined.

(3) All vehicles are homogeneous in parameters, including type, battery capacity, and maximum load capacity.

(4) Each vehicle departs from and ultimately returns to the central depot.

(5) The total demand on any route shall not exceed a vehicle's maximum cargo capacity.

(6) Vehicle speeds are assumed constant, and traffic congestion effects are disregarded.

ISSN: 2688-8645

(7) The remaining battery charge remains non-negative throughout the delivery process.

2.2. Cost Analysis

2.2.1. Transportation Cost

The transportation cost of vehicles is composed of fixed cost and variable cost. The fixed cost includes the start-up cost of the vehicle, while the variable cost includes the transportation cost of the vehicle, which is related to the distance of the node. Total transportation cost is calculated by:

$$\min C_1 = w_1 \sum_{k=1}^{m} x_k + w_2 \sum_{i=0}^{n} \sum_{j=0}^{n} \sum_{k=1}^{m} d_{ij} X_{ijk}, \tag{1}$$

where w_1 is the fixed cost per vehicle and x_k is the number of vehicles. w_2 represents the transportation cost per kilometer, d_{ij} is the distance from node i to node j, X_{ijk} is the decision variable, if an arc (i, j) is traveled, $X_{ijk} = 1$, otherwise $X_{ijk} = 0$.

2.2.2. Battery Degradation Cost

Battery degradation occurs during the charging process of electric vehicles, with capacity loss varying depending on the depth of discharge and cumulative battery throughput capacity. A cycle degradation model under varying depth of discharge is established by [32]:

$$E_{loss}(10\% \geq D \geq 50\%) = \left(\gamma_1 \cdot D^2 + \gamma_2 \cdot D + \gamma_3\right) \cdot \eta \cdot Ah^{0.87}, \tag{2}$$

$$E_{loss}(10\% < D, D > 50\%) = \left(\alpha_3 \cdot \exp\left(\beta_3 \cdot D\right) + \alpha_4 \cdot \exp\left(\beta_4 \cdot D\right)\right) \cdot \eta \cdot Ah^{0.65}, \tag{3}$$

where E_{loss} is percentage of capacity loss due to cyclic degradation, D is the discharge depth, Ah represents cumulative battery throughput capacity. $\gamma_1, \gamma_2, \gamma_3, \beta_3, \beta_4, \alpha_3, \alpha_4$ are constant fitting parameters. η is the static degradation acceleration factor, typically set to 1.

The battery demand for a single trip is calculated to

$$E_d = d_{ij} \cdot h_{eff}, \tag{4}$$

where E_d determined by driving distance d_{ij} and electric energy consumption per unit distance h_{eff}.

Depth of discharge is calculated to

$$D = \frac{E_d}{Q} = \frac{d_{ij} \cdot h_{eff}}{Q}. \tag{5}$$

Combined with the nonlinear relationship in the cycle degradation formula, the degradation cost coefficient ε of the battery per unit distance is obtained,

$$\varepsilon_1(10\% \geq D \geq 50\%) = \gamma_1 \cdot \left(\frac{d_{ij} \cdot h_{eff}}{Q}\right)^2 + \gamma_2 \cdot \left(\frac{d_{ij} \cdot h_{eff}}{Q}\right) + \gamma_3, \tag{6}$$

$$\varepsilon_2(10\% < D, D > 50\%) = \alpha_3 \cdot \exp\left(\beta \cdot \frac{d_{ij} \cdot h_{eff}}{Q}\right) + \alpha_4 \cdot \exp\left(\beta_4 \cdot \frac{d_{ij} \cdot h_{eff}}{Q}\right), \tag{7}$$

Then , a mathematical model of battery degradation cost is defined as follows,

$$\min C_2 = \frac{\varepsilon}{100} \cdot \frac{E_d}{Ah} \cdot E_{bat}. \tag{8}$$

2.2.3. Charging Cost

The charging cost is calculated based on a fixed electricity price and the amount of energy required for vehicle recharging. During charging, a portion of energy is converted into heat or lost in other forms, causing the actual energy drawn from the grid to exceed the energy stored in the battery. For lithium batteries, the charging efficiency typically ranges from 85% to 95% [33]. The charging cost is expressed as

$$\min C_3 = p \cdot \frac{E_d}{\omega}, \tag{9}$$

p is electricity price, ω indicates the charging efficiency.

Therefore, the mathematical model of ECVRP is formulated as a mixed-integer program as follows:

$$\min T = C_1 + C_2 + C_3 \tag{10}$$

$$\sum_{i \in N}^{n} X_{ijk} = 1, \forall j \in N, \forall k \in K, \tag{11}$$

$$0 < Q_{0jk} < Q, \forall j \in N, \forall k \in K, \tag{12}$$

$$\sum_{k=0}^{m} X_{0jk} = \sum_{k=0}^{m} X_{j0k}, \forall j \in N, \forall k \in K, \tag{13}$$

$$\sum_{i=0}^{n} X_{i0k} = \sum_{j=0}^{n} X_{0jk} = 1, \forall k \in K, \tag{14}$$

$$\sum_{i=0}^{n} X_{ij} = \sum_{j=0}^{n} X_{ji}, \forall i \in V, \forall j \in V, i \neq j, \tag{15}$$

$$\sum_{i=0}^{n} X_{ijk} \leq \sum_{k=1}^{m} Y_{kr}, \forall k \in K, r \in R, \tag{16}$$

$$q_{kr}^{2} = Q, \forall k \in K, \tag{17}$$

$$P_{ik} = \left(B_c - E_{ik}\right) \cdot Y_{kb}. \tag{18}$$

The objective to minimize the transportation cost is defined in Constraint (10). Constraint (11) ensures that each demand point is served by only one vehicle. Constraint (12) describes the capacity limit of the vehicle. Constraint (13) guarantees that each EV departs from and returns to the central depot. Constraints (14) and (15) enforce that each vertex maintains equal numbers of incoming and outgoing arcs. Constraint (16) emphasizes that vehicle is charged at the charging station. Constraint (17) indicates that the vehicle is fully charged when leaving the charging station r. Constraint (18) specifies a full charge strategy.

3. Hybrid Genetic Neighborhood Search Algorithm for ECVRP

This section proposes a hybrid genetic neighborhood search algorithm for the ECVRP. While conventional genetic algorithms are effective in global exploration, they often converge prematurely to local optima and exhibit slow convergence rates, especially when addressing high-dimensional constraints. The hybrid genetic neighborhood search algorithm integrates global search with adaptive local refinement to achieve improved solution quality and convergence performance. Specifically, the HGNSA algorithm adopts an improved elite preservation strategy as the selection operator, followed by an enhanced crossover operator, and finally applies multiple neighborhood search strategies as an improved mutation operator to optimize the population. The pseudo-code of the proposed HGNSA algorithm is presented in Table 1.

Table 1. The pseudo-code of the proposed HGNSA algorithm

ALGORITHM HGNSA
Input: the initialize population $X_{0,i} = \{x_{0,1}, x_{0,2}, \dots, x_{0,n}\}$
Evaluate $F(X_{0,i})$
$s\_best \leftarrow \min(x_{0,i})$
While $seg \le \max\_seg$ **do**
While $iter \le seg$ **do**
$[Z_{01}, Z_{02}, Z_{03}] \leftarrow$ rank and split (Z)
If $x_{0,i} \in Z_{01}$ **then**
$x'_{0,i} \leftarrow x_{0,i}$;
Else if $x_{0,i} \in Z_{02}$ **then**
$x_{0,i} crossover Z_{01}$, $x'_{0,i} \leftarrow x_{0,i}$;
Else
$x_{0,i} \leftarrow random, x'_{0,i} \leftarrow x_{0,i}$
End if
Mutation operation
Neighborhood search operation
Forming a new population, $X_{1,i} = \{x_{1,1}, x_{1,2}, \dots, x_{1,n}\}$.
$iter \leftarrow iter + 1$
End while
Sort the new population based on fitness and perform operations
$seg \leftarrow seg + 1$
End while
Output: the best solution s^*

3.1. Encoding and Decoding

To address vehicle routing problems with dual constraints of vehicle capacity and battery capacity, this study adopts a natural number encoding scheme combined with an adaptive split mechanism. In the chromosome structure, customer nodes are represented by positive integers, the central depot is encoded as 0, and charging stations are encoded as C. The chromosome sequence indicates the visiting order of customer nodes. During the decoding phase, customer nodes are sequentially assigned to vehicle routes. When the vehicle reaches its capacity limit, a depot (0) is inserted to end the current route and start a new one. If the remaining battery capacity is insufficient to reach the next customer or complete the route, a charging station (C) is inserted before continuing. Each sub-route is enclosed by depot nodes at both ends, ensuring feasibility and compliance with operational constraints.

For example, given the initial chromosome sequence [2, 3, 5, 1, 4], the vehicle first visits customer nodes 2 and 3. Upon reaching node 3, the vehicle reaches its capacity limit and returns to the central depot (0). A new vehicle is then dispatched to continue the route. When it reaches customer node 5, the remaining battery is insufficient to reach the next customer, so a charging station (C) is inserted. After charging, the vehicle proceeds to serve customer nodes 1 and 4, and finally returns to the depot. As a result, two routes are generated: [0, 2, 3, 0] and [0, 5, C, 1, 4, 0].

ISSN: 2688-8645

3.2. Initial Population Generation

To avoid slow convergence caused by poor initial population quality and premature convergence resulting from overly optimal initial solutions, a stochastic method is employed to generate the initial population. Specifically, a randomized sequence of customer nodes is first created and then partitioned into feasible routes using a split algorithm that considers both vehicle capacity and battery constraints. This process is repeated multiple times to construct a diverse initial population. By combining randomness with feasibility, this approach expands the search space and promotes balanced exploration of various routing configurations, thereby reducing the risk of premature convergence in subsequent optimization stages.

3.3. Fitness Evaluation

The fitness value of each chromosome determines its probability of being selected during the evolutionary process, with higher fitness values indicating better solutions. Since the objective of the ECVRP is to minimize the total logistics cost—including transportation, charging, and battery degradation—the fitness function is defined to be inversely proportional to the total objective value:

$$Fitness(S) = \frac{1}{T_{\min} + \sigma}, \tag{19}$$

where T is the total cost of solution, and $\sigma = 10^{-6}$ prevents division by zero. This formulation prioritizes solutions with lower costs while maintaining numerical stability during selection operations.

3.4. Selection Operator

This study proposes a novel selection operator based on an elite preservation strategy. The fitness values of all chromosomes are calculated using a predefined fitness function and subsequently ranked. The top-ranked solutions are designated as elites, which retain more chromosome segments to enhance their transmission probability in the evolutionary process. For non-elite solutions, crossover operations are performed between normalized probabilistic candidates and elites, while inferior solutions are systematically replaced by randomly generated new individuals to form an optimized population. This approach ensures both the inheritance of high-quality chromosome segment and the maintenance of population diversity.

The specific selection process is as follows.

Step1: The decline probability is calculated by

$$P(i) = \frac{k}{i} \tag{20}$$

Step2: The normalization constant is determined by

$$S = \sum_{i=1}^{n} \frac{1}{i} \tag{21}$$

$$k = \frac{1}{S} \tag{22}$$

Step3: Calculate the number of mating between each elite individual and ordinary individual.

$$N_i = P(i) \cdot m \tag{23}$$

$$P(i) = \frac{k}{i} = \frac{\frac{1}{S}}{i} = \frac{1}{iS} \tag{24}$$

$$N_i = \frac{1}{iS} \cdot m \tag{25}$$

ISSN: 2688-8645

Step4: The range of individuals assigned is

$$R_i = \left(\sum_{j=10}^{i-1} N_j + 1, \sum_{j=1}^{i} N_j\right) \tag{26}$$

Table 2. Parameters of the normalization formula

Parameters	
n	Number of elite individuals
m	Number of ordinary individuals
$P(i)$	Probability of the *i*-th excellent individual
k	Normalize the constant so that the sum of all probabilities is 1
S	Sum of harmonic series
N_i	The number of crossover between the *i*-th elite individual and non-elite individuals
R_i	The crossover scope of the *i*-th elite individual with non-elite individuals

3.5. Crossover Operator

To enhance the inheritance of high-quality chromosome segments from elite individuals while maintaining population diversity, this study defines the crossover range for each elite individual based on Eq. (26). The operator dynamically extracts gene fragments from parent chromosomes in proportion to their fitness values. Then these fragments are mapped onto ordinary solutions through a structured recombination process, ensuring that offspring inherit advantageous traits while reducing the risk of premature convergence. Subsection 3.6, Steps 3 to 7, provides a detailed description of the crossover process.

3.6. Mutation Operator

Due to the strong randomness and limited local search capability of genetic algorithms, this study incorporates neighborhood search as an enhanced mutation operator. The integration of genetic algorithms with neighborhood search significantly improves both solution quality and convergence speed. The mutation phase employs four neighborhood search strategies: the maximum-distance destruction operator, the 2-opt method, random exchange, and the optimal single-point insertion method.

3.6.1. Maximum Distance Destruction Operator

This operator enhances exploration by destructing route segments with the largest travel distances between adjacent customer nodes. Specifically, for a given route, the distance between each pair of adjacent customer nodes is expressed as $D_N = d_{n-1,n}$. Sorted in descending order and calculate the distance between adjacent points of the path to get the set $D = [D_1, D_2, \ldots, D_N]$. The top 30% of node pairs with the greatest distances are selected, and the corresponding nodes are removed from the current solution. These removed nodes are then reinserted into the route at random feasible positions. This destruction-reconstruction process accelerates the search for improved solutions by targeting inefficient segments and increasing solution diversity.

3.6.2. 2-opt Method

The 2-opt method is a classical local search operator used to eliminate route crossings and reduce total travel distance. It operates by iteratively selecting two non-adjacent edges in a route and reversing the sequence of nodes between them. This reversal replaces two edges that form a crossing with two new edges that eliminate the intersection, yielding a shorter and more efficient route.

3.6.3. Random Exchange

The random exchange operator enhances population diversity by stochastically perturbing existing routes. Two distinct customer nodes are randomly selected from the current solution, and their positions are swapped to generate a new route configuration. This operation expands the search space by introducing random variations and enables the algorithm to escape from local optima. Although the change does not always result in immediate improvement, it maintains solution diversity and supports global exploration.

3.6.4. Optimal Single Point Insertion Method

The optimal single-point insertion method is a greedy heuristic that optimizes the placement of individual nodes within a route. Randomly remove a node and insert it into the optimal position to minimize the total distance increase. Given the current route $P=[v_1,v_2,\ldots,v_n]$, select uniformly at random a non-terminal node $v_r(1<r\le k-2)$. Denote by $P^{'}=[v_1,v_2,\ldots,v_{r-1},v_{r+1},\ldots v_n]$. The sequence obtained by removing v_r. For each insertion index $i(1\le i\le \left|P^{'}\right|)$, compute the incremental distance $\Delta_i=d_{P^{'}[i-1],n_r}+d_{n_r,P^{'}[i]}-d_{P^{'}[i-1],P^{'}[i]}$. Let i_{best} inserting v_r between $P^{'}\left[i-1\right]$ and $P^{'}\left[i\right]$ then yields the new route $P_{new}=\left[v_1,v_2,\ldots,P^{'}\left[i_{best}-1\right],v_r,P^{'}\left[i_{best}\right]\ldots v_n\right]$.

3.7. Model Solution Procedure

Based on the main algorithm description, the solution procedure for the ECVRP model is as follows.

Step1: For the convenience of research, initial feasible solutions N are randomly generated, and the set $X_{0,i}=\left\{x_{0,1},x_{0,2},\ldots,x_{0,n}\right\}$ is generated.

Step2: Calculate the fitness function of the initial feasible solution. Since the fitness function requires the minimum, the initial feasible solution is sorted in reverse order to generate $X^{'}_{0,i}=\left\{x^{'}_{0,1},x^{'}_{0,2},\ldots,x^{'}_{0,n}\right\}$.

Step3: The elite, general, and inferior solution sets are recorded as $Z_{01}=\left\{x^{'}_{0,1},x^{'}_{0,2},\ldots,x^{'}_{\|N\cdot 10\%+1\|}\right\}$, $Z_{02}=\left\{x^{'}_{\|N\cdot 10\%+2\|},x^{'}_{\|N\cdot 10\%+3\|},\ldots,x^{'}_{\|N\cdot 90\%-1\|}\right\}$, and $Z_{03}=\left\{x^{'}_{\|N\cdot 90\%\|},x^{'}_{\|N\cdot 90\%+1\|},\ldots,x^{'}_{N}\right\}$, respectively.

Step4: If $x_{i,j}\subseteq Z_{01}$, then Z_{01} keep $x_{i,j}$ as an elite individual. If $x_{i,j}\subseteq Z_{02}$, then $x_{i,j}$ crosses with the individual in Z_{01} according to step 6. If $x_{i,j}\subseteq Z_{03}$, then generate a new random solution and form a new set $Z^{'}_{03}$.

Step5: The individual in Z_{02} according to Eq.(25) calculate the probability of crossover with each excellent individual.

Step6: The elite individuals in Z_{01} retain some chromosome fragments according to the normalization formula, and the unreserved chromosome fragments are inserted by the Z_{02} individuals in reverse order to generate a new set $Z^{'}_{02}$.

Step7: The new population $X_{1,i}=\left\{x_{1,1},x_{1,2},\ldots,x_{1,n}\right\}$ is formed by combining Z_{01}, $Z^{'}_{02}$ and $Z^{'}_{03}$, and the next iteration proceeds. Specifically, since the individual of the first set Z_{01} remains, a new set $Z^{'}_{01}$ is generated only if the second iteration completes reordering.

Step8: Evaluate the objective function for the final population $X_{100,i}$. $x_{100,1}$ is generated by sorting.

Step9: Output the result. The iteration is stopped until the number of iterations is completed. Then, output s^* .

4. Numerical Experiments and Case Analysis

Table 3. The parameters used in the HGNSA algorithm.

Description	Parameter	Numerical value
Algorithm parameters	Mutation probability	0.1
	Crossover probability	0.8
	Population size	500
	Population selection number	100
Model parameters	Electricity price	0.527
	Unit distance cost	0.22
	Battery cost	100000
	Battery degradation rate	10
	Charging efficiency	90
	Vehicle start-up cost	100
	Ah	5000
	Power consumption per km	13.5

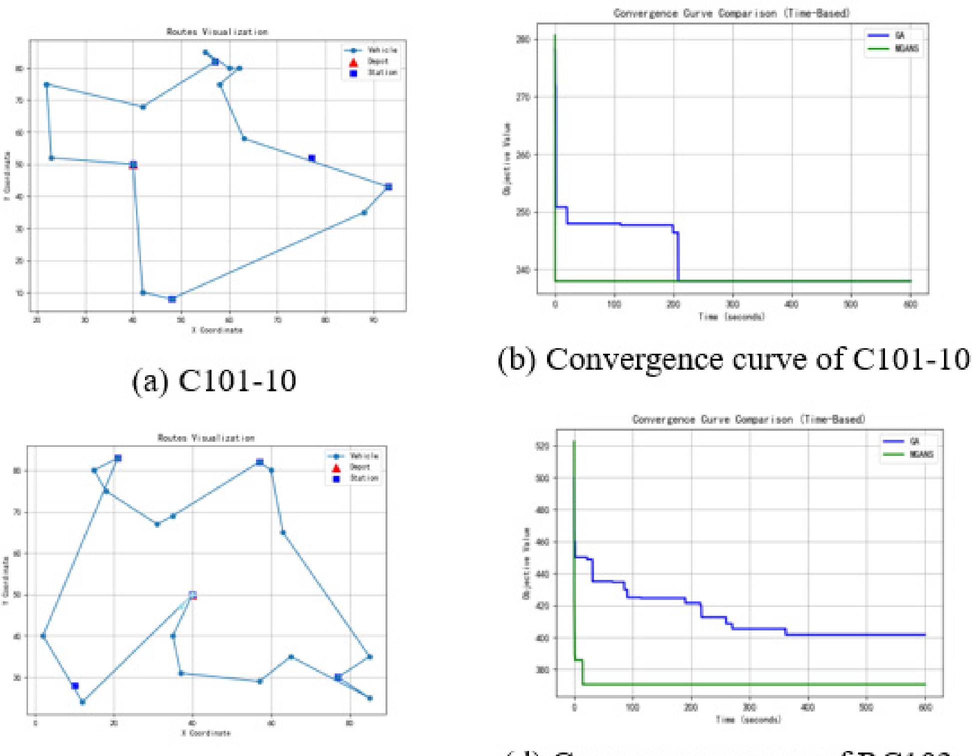

(a) C101-10

(b) Convergence curve of C101-10

(c) RC103-15

(d) Convergence curve of RC103-15

Fig 1. Comparison between the optimal route generated by HGNSA and the convergence performance of HGNSA versus GA

In this section, to verify the performance of the HGNSA, the computational experiments are conducted. This study addresses the ECVRP using an improved HGNSA based on a newly proposed cost model, and compares its solution quality with that of the classical GA. The improved and classical GA algorithm is implemented in Python. All experiments are conducted on a PC with Intel Core i5-9300H CPU and 16 GB RAM.

Therefore, this study employs Schneider's EVRPTW dataset for computational experiments [14]. This dataset based on the Solomon benchmark instances, comprises two sets of benchmark instances: 56 large-scale instances and 36 small-scale instances [15]. Given the focus on small-scale port scenarios, the small-scale benchmark instances were selected for experimental analysis. The dataset categorizes instances into three groups based on customer geographic distribution: random customer distribution (R), clustered customer distribution (C), and a mixture of both (RC). Additionally, instances are classified into the 100-series and 200-series according to time window lengths. Since time window constraints are easily satisfied in the target scenarios, instances C2, R2, and RC2 were excluded from the analysis [34].

Table 3 presents the values of all parameters utilized in the HGNSA algorithm. The values of some parameters are derived from previous studies, and the values of other parameters are determined in combination with the actual situation [14,32,33,35,36].

Fig. 1 illustrates the route planning results and convergence behavior of the proposed HGNSA algorithm using two benchmark instances, C101-10 and RC103-15, as representative examples. Subfigures (a) and (c) present the optimized routes for instances C101-10 and RC103-15, respectively, highlighting the vehicle paths, depot, and charging station locations. Subfigures (b) and (d) compare the convergence curves of HGNSA and the traditional GA on instances C101-10 and RC103-15, demonstrating that HGNSA achieves faster convergence and better final solution quality within the same runtime.

Table 4. Results of ECVRP instances (the best results)

Ins.	GA			HGNSA			Deviation
	TD	TC	S	TD	TC	S	ΔS (%)
C101-5	184.19	196.95	0.46	184.19	196.95	0.02	-95.65%
C103-5	147.97	177.07	0.39	147.97	177.07	0.02	-94.87%
R104-5	136.69	173.02	0.37	136.69	173.02	0.02	-94.59%
R105-5	153.01	181.74	0.8	153.01	181.74	0.02	-97.50%
RC105-5	207.64	213.03	0.39	207.64	213.03	0.02	-94.87%
RC108-5	207.53	210.36	0.32	207.53	210.36	0.03	-90.63%
C101-10	256.26	237.97	170.26	256.26	237.97	0.2	-99.88%
C104-10	277.54	251.05	310.3	277.54	251.05	0.43	-99.86%
R102-10	220.27	220.66	324.66	220.27	220.66	16.95	-94.78%
R103-10	153.82	280.08	302.77	153.82	280.08	7.42	-97.55%
RC102-10	354.31	293.46	132.49	354.31	293.46	0.61	-99.54%
RC108-10	322.36	274.11	142.35	322.36	274.11	0.34	-99.76%
C103-15	282.33	348.65	600	**273.52**	**344.34**	22.17	-96.31%
C106-15	216.35	216.95	600	216.35	216.95	26.76	-95.54%
R102-15	256.8	239.6	560.76	256.8	239.6	22.27	-96.03%
R105-15	257.96	337.02	582.01	**253.19**	**335.48**	5.51	-99.05%
RC103-15	319	372.19	600	**318.24**	**370.57**	13.97	-97.67%
RC108-15	353.73	383.35	584.38	353.73	383.35	12.19	-97.91%

Table 4 presents the best solutions obtained by both the GA and HGNSA algorithms within a time limit of 600 seconds. It is observed that, across all benchmark instances, the HGNSA algorithm consistently achieves equal or lower objective function values compared to the GA algorithm. Specifically, in instances such as C103-15, R105-15, and RC103-15, HGNSA shows a significant reduction in total distance and total cost, confirming its superior global search ability. This indicates that the incorporation of neighborhood search strategies effectively mitigates the premature convergence observed in conventional GA and enhances the exploration of promising solution regions.

Fig. 2 compares the runtime performance of HGNSA and the traditional GA across all test cases. The results indicate that HGNSA achieves noticeably faster solving speed in small-scale instances. It also consistently converges more quickly and yields higher-quality solutions in these cases, demonstrating its effectiveness in handling simpler problems with greater efficiency.

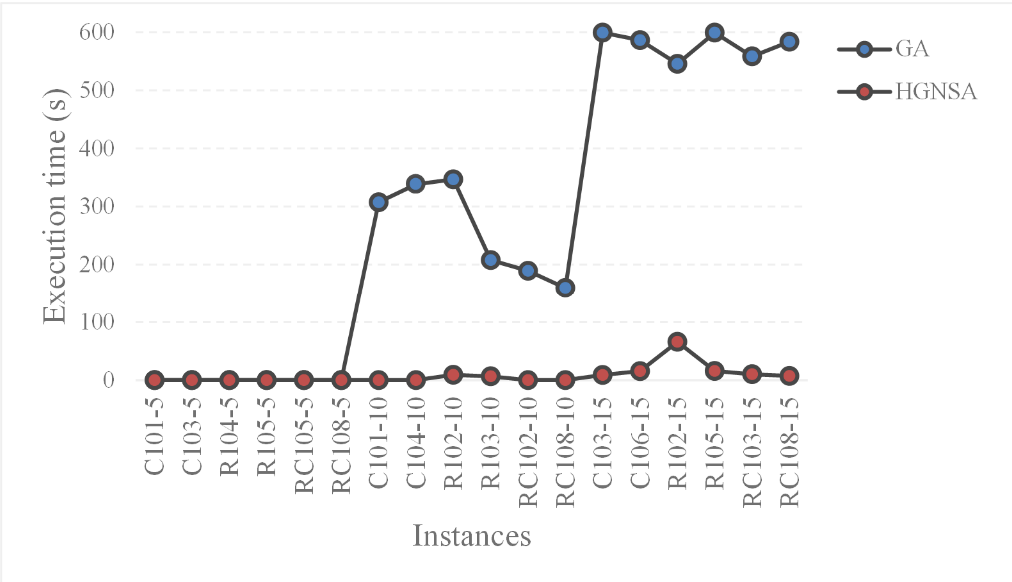

Fig 2. Comparison of runtime performance between HGNSA and GA on all test instances

Table 5 further reports the average results of 10 independent runs for each instance. Observing from the table, the HGNSA consistently outperforms the GA in both average total distance and average total cost. Notably, for small-scale instances with 5 customer nodes, both GA and HGNSA are able to quickly identify the optimal route. However, as the problem size increases to 10 and 15 customer nodes, the GA fails to consistently find the optimal solution and exhibits a noticeable increase in runtime. For example, in R102-15, HGNSA achieves a 5.94% reduction in average total distance and a 3.92% reduction in average total cost compared to the GA. This consistent performance highlights the robustness of the HGNSA algorithm against random fluctuations during initialization and evolutionary processes.

Overall, the experimental results confirm that the proposed HGNSA algorithm not only achieves better optimization performance but also demonstrates improved stability over multiple runs, making it a reliable and effective approach for solving the ECVRP under complex operational constraints.

Interestingly, in certain benchmark instances, it was observed that longer routes sometimes led to lower total transportation costs. This phenomenon results from the introduction of battery degradation cost in the objective function. A longer route that avoids frequent charging station stops often results in reduced cumulative battery throughput and thus lower capacity loss, despite incurring a slightly higher transport distance. This highlights the effectiveness of HGNSA in balancing different cost components, and demonstrates that the shortest route is not always the most cost-efficient when considering battery health and operational sustainability.

Table 5. Results of ECVRP instances (the average results)

Ins.	GA			HGNSA			Deviation		
	ASTD	ASTC	S(s)	ASTD	ASTC	S(s)	ΔTD (%)	ΔTC (%)	ΔS (%)
C101-5	184.19	196.95	1.00	184.19	196.95	1.00	0.00%	0.00%	0.00%
C103-5	147.97	177.07	1.00	147.97	177.07	1.00	0.00%	0.00%	0.00%
R104-5	136.69	173.02	1.00	136.69	173.02	1.00	0.00%	0.00%	0.00%
R105-5	153.01	181.74	1.00	153.01	181.74	1.00	0.00%	0.00%	0.00%
RC105-5	207.64	213.03	1.00	207.64	213.03	1.00	0.00%	0.00%	0.00%
RC108-5	207.53	210.36	1.00	207.53	210.36	1.00	0.00%	0.00%	0.00%
C101-10	256.31	238.00	307.95	256.26	237.97	1.00	-0.02%	-0.01%	-99.68%
C104-10	280.09	252.15	339.03	277.54	251.05	1.00	-0.91%	-0.44%	-99.71%
R102-10	221.87	221.15	347.40	220.27	220.66	10.10	-0.72%	-0.22%	-97.09%
R103-10	154.40	280.35	208.43	153.82	280.08	7.42	-0.38%	-0.09%	-96.44%
RC102-10	354.31	293.46	189.92	354.31	293.46	1.00	0.00%	0.00%	-99.47%
RC108-10	322.36	274.11	160.23	322.36	274.11	1.00	0.00%	0.00%	-99.38%
C103-15	318.44	367.29	600.00	273.52	344.34	9.72	-14.11%	-6.25%	-98.38%
C106-15	226.84	222.31	587.26	216.35	216.95	16.46	-4.63%	-2.41%	-97.20%
R102-15	277.19	251.34	546.44	260.74	241.50	66.80	-5.94%	-3.92%	-87.78%
R105-15	282.46	351.86	600.00	254.10	335.78	16.64	-10.04%	-4.57%	-97.23%
RC103-15	355.12	391.55	559.20	318.92	372.03	11.07	-10.19%	-4.99%	-98.02%
RC108-15	375.74	407.30	584.38	353.73	383.35	8.16	-5.86%	-5.88%	-98.60%

5. Conclusion

This study investigates the ECVRP considering battery degradation and proposes a novel hybrid algorithm, HGNSA, which combines the global exploration capability of the GA with the local exploitation of neighborhood search. In this algorithm, we apply split method to the encoding and decoding process and improve the selection, crossover, and mutation operations of traditional GA algorithms. The experimental results demonstrate that HGNSA consistently outperforms the standard GA in terms of both the best solution found within a fixed computational time and the average performance across multiple independent runs.

Specifically, HGNSA achieves lower total cost and total distance in all test instances, while also demonstrating improved stability as evidenced by the significantly reduced standard deviation. These results confirm the superiority of HGNSA in balancing global search and local refinement, effectively avoiding premature convergence and enhancing solution quality. In the current study focusing on small-scale benchmark instances, HGNSA exhibits clear advantages in both convergence speed and solution quality.

Overall, HGNSA proves to be a promising approach for solving ECVRP instances, offering both efficiency and robustness in practical applications.

Acknowledgments

Thanks for the Research Project on Graduate Education and Teaching Reform at Shandong Jiaotong University (JYY202221), and in part by Undergraduate Teaching Reform Research Project of Shandong Jiaotong University (2023YB42).

References

[1] Erdelić T, Carić T. A survey on the electric vehicle routing problem: variants and solution approaches[J]. Journal of Advanced Transportation, 2019, 2019(1): 5075671.

[2] Zhao J, Zeng Z, Liu Y. Electric vehicle routing problem considering traffic conditions and real-time loads[J]. Transportation Research Part C: Emerging Technologies, 2025, 176: 105150.

[3] Vakili S, Ölçer A I. Techno-economic-environmental feasibility of photovoltaic, wind and hybrid electrification systems for stand-alone and grid-connected port electrification in the Philippines[J]. Sustainable cities and society, 2023, 96: 104618.

[4] Zhu S, Mac Kinnon M, Soukup J, et al. Assessment of the greenhouse gas, Episodic air quality and public health benefits of fuel cell electrification of a major port complex[J]. Atmospheric Environment, 2022, 275: 118996.

[5] Zhang S, Gajpal Y, Appadoo S S, et al. Electric vehicle routing problem with recharging stations for minimizing energy consumption[J]. International journal of production economics, 2018, 203: 404-413.

[6] Kennedy B, Patterson D, Camilleri S. Use of lithium-ion batteries in electric vehicles[J]. Journal of Power Sources, 2000, 90(2): 156-162.

[7] Lai X, Chen Q, Tang X, et al. Critical review of life cycle assessment of lithium-ion batteries for electric vehicles: A lifespan perspective[J]. Etransportation, 2022, 12: 100169.

[8] Dantzig G B, Ramser J H. The truck dispatching problem[J]. Management Science, 1959, 6(1): 80-91.

[9] Laporte G, Nobert Y. A branch and bound algorithm for the capacitated vehicle routing problem[J]. Operations-Research-Spektrum, 1983, 5: 77-85.

[10] Kolen A W J, Rinnooy Kan A H G, Trienekens H W J M. Vehicle routing with time windows[J]. Operations Research, 1987, 35(2): 266-273.

[11] Erdoğan S, Miller-Hooks E. A green vehicle routing problem[J]. Transportation Research Part E: Logistics and Transportation Review, 2012, 48(1): 100-114.

[12] Kucukoglu I, Dewil R, Cattrysse D. The electric vehicle routing problem and its variations: A literature review[J]. Computers & Industrial Engineering, 2021, 161: 107650.

[13] Schneider M, Stenger A, Goeke D. The electric vehicle-routing problem with time windows and recharging stations[J]. Transportation Science, 2014, 48(4): 500-520.

[14] Solomon M M. Algorithms for the vehicle routing and scheduling problems with time window constraints[J]. Operations Research, 1987, 35(2): 254-265.

[15] He S Y, Kuo Y H, Wu D. Incorporating institutional and spatial factors in the selection of the optimal locations of public electric vehicle charging facilities: A case study of Beijing, China[J]. Transportation Research Part C: Emerging Technologies, 2016, 67: 131-148.

[16] Sadati M E H, Akbari V, Çatay B. Electric vehicle routing problem with flexible deliveries[J]. International Journal of Production Research, 2022, 60(13): 4268-4294.

[17] Erdelić T, Carić T, Erdelić M, et al. Electric vehicle routing problem with single or multiple recharges[J]. Transportation Research Procedia, 2019, 40: 217-224.

[18] Lu J, Chen Y, Hao J K, et al. The time-dependent electric vehicle routing problem: Model and solution[J]. Expert Systems with Applications, 2020, 161: 113593.

[19] Mao H, Shi J, Zhou Y, et al. The electric vehicle routing problem with time windows and multiple recharging options[J]. IEEE Access, 2020, 8: 114864-114875.

[20] Wang Y, Zhou J, Sun Y, et al. Collaborative multidepot electric vehicle routing problem with time windows and shared charging stations[J]. Expert Systems with Applications, 2023, 219: 119654.

[21] Liu K, Hu X, Yang Z, et al. Lithium-ion battery charging management considering economic costs of electrical energy loss and battery degradation[J]. Energy Conversion and Management, 2019, 195: 167-179.

[22] Wang J, Kang L, Liu Y. Optimal scheduling for electric bus fleets based on dynamic programming approach by considering battery capacity fade[J]. Renewable and Sustainable Energy Reviews, 2020, 130: 109978.

[23] Li L, Dong S, Wang L. Capacity degradation prediction of electric vehicle battery by integrating convolutional neural network with informer model[J]. Journal of Power Sources, 2025, 651: 237497.

[24] Yu K, Yan P, Liu Y, et al. Battery degradation mitigation-oriented strategy for optimizing e-hailing electric vehicle operations[J]. Transportation Research Part E: Logistics and Transportation Review, 2025, 196: 104006.

[25] Ou S. Estimate long-term impact on battery degradation by considering electric vehicle real-world end-use factors[J]. Journal of Power Sources, 2023, 573: 233133.

[26] Zhang S, Chen M, Zhang W, et al. Fuzzy optimization model for electric vehicle routing problem with time windows and recharging stations[J]. Expert Systems with Applications, 2020, 145: 113123.

[27] Hien V Q, Dao T C, Binh H T T. A greedy search based evolutionary algorithm for electric vehicle routing problem[J]. Applied Intelligence, 2023, 53(3): 2908-2922.

[28] Souza A L S, Papini M, Penna P H V, et al. A flexible variable neighbourhood search algorithm for different variants of the Electric Vehicle Routing Problem[J]. Computers & Operations Research, 2024, 168: 106713.

[29] Duman E N, Taş D, Çatay B. A bidirectional branch-and-price algorithm with Pulse procedure for the Electric Vehicle Routing Problem with flexible deliveries[J]. Transportation Research Part C: Emerging Technologies, 2024, 165: 104699.

[30] Yang S, Zhang R, Ma Y, et al. Adaptive large neighborhood search incorporating mixed-integer linear programming for electric vehicle routing problem with mobile charging and nonlinear battery degradation[J]. Applied Soft Computing, 2025, 175: 112988.

[31] İslim R B, Çatay B. An effective matheuristic approach for solving the electric traveling salesperson problem with time windows and battery degradation[J]. Engineering Applications of Artificial Intelligence, 2024, 132: 107943.

[32] Sarasketa-Zabala E, Gandiaga I, Martinez-Laserna E, et al. Cycle ageing analysis of a LiFePO4/graphite cell with dynamic model validations: Towards realistic lifetime predictions[J]. Journal of Power Sources, 2015, 275: 573-587.

[33] Rydh C J, Sandén B A. Energy analysis of batteries in photovoltaic systems. Part I: Performance and energy requirements[J]. Energy conversion and management, 2005, 46(11-12): 1957-1979.

[34] Duman E N, Taş D, Çatay B. Branch-and-price-and-cut methods for the electric vehicle routing problem with time windows[J]. International Journal of Production Research, 2022, 60(17): 5332-5353.

[35] Cataldo-Díaz C, Linfati R, Escobar J W. Mathematical model for the electric vehicle routing problem considering the state of charge of the batteries[J]. Sustainability, 2022, 14(3): 1645.

[36] Miri I, Fotouhi A, Ewin N. Electric vehicle energy consumption modelling and estimation—A case study[J]. International Journal of Energy Research, 2021, 45(1): 501-520.